A novel mechanism of sodium iodide symporter repression in differentiated thyroid cancer

Vicki E. Smith[1], Martin L. Read[1], Andrew S. Turnell[2], Rachel J. Watkins[1], John C. Watkinson[1], Greg D. Lewy[1], Jim C. W. Fong[1], Sally R. James[1], Margaret C. Eggo[1], Kristien Boelaert[1], Jayne A. Franklyn[1] and Christopher J. McCabe[1,*]

[1]School of Clinical and Experimental Medicine, Institute of Biomedical Research and [2]School of Cancer Sciences, University of Birmingham, B15 2TH, UK

*Author for correspondence (mccabcjz@bham.ac.uk)

Accepted 13 June 2009
Journal of Cell Science 122, 3393-3402 Published by The Company of Biologists 2009
doi:10.1242/jcs.045427

Summary

Differentiated thyroid cancers and their metastases frequently exhibit reduced iodide uptake, impacting on the efficacy of radioiodine ablation therapy. PTTG binding factor (PBF) is a proto-oncogene implicated in the pathogenesis of thyroid cancer. We recently reported that PBF inhibits iodide uptake, and have now elucidated a mechanism by which PBF directly modulates sodium iodide symporter (NIS) activity in vitro. In subcellular localisation studies, PBF overexpression resulted in the redistribution of NIS from the plasma membrane into intracellular vesicles, where it colocalised with the tetraspanin CD63. Cell-surface biotinylation assays confirmed a reduction in plasma membrane NIS expression following PBF transfection compared with vector-only treatment. Coimmunoprecipitation and GST-pull-down experiments demonstrated a direct interaction between NIS and PBF, the functional consequence of which was assessed using iodide-uptake studies in rat thyroid FRTL-5 cells. PBF repressed iodide uptake, whereas three deletion mutants, which did not localise within intracellular vesicles, lost the ability to inhibit NIS activity. In summary, we present an entirely novel mechanism by which the proto-oncogene PBF binds NIS and alters its subcellular localisation, thereby regulating its ability to uptake iodide. Given that PBF is overexpressed in thyroid cancer, these findings have profound implications for thyroid cancer ablation using radioiodine.

Supplementary material available online at
http://jcs.biologists.org/cgi/content/full/122/18/3393/DC1

Key words: PBF, NIS, Iodide uptake, Thyroid cancer

Introduction

The sodium iodide symporter (NIS) is an integral membrane glycoprotein located in the basolateral plasma membrane of thyroid follicular epithelial cells. NIS is responsible for mediating iodide uptake and is consequently essential for thyroid hormone synthesis in thyroid cells. The ability of the thyroid to accumulate radioiodine has long been used to image and treat tumours of the thyroid and their metastases, distinguishing NIS as both a diagnostic and a therapeutic tool (Boelaert and Franklyn, 2003).

Thyroid carcinomas are the most common endocrine neoplasm and their annual incidence is rising (Ries et al., 2008). Although most differentiated thyroid carcinomas have a good prognosis, up to 35% recur (Mazzaferri and Kloos, 2001). Crucially, many thyroid cancers and their metastases demonstrate reduced iodide uptake in comparison to normal thyroid tissue and, even after thyrotrophin (thyroid-stimulating hormone, TSH) stimulation, 10-20% of these tumours are unable to concentrate enough radioiodine for effective therapy (Kogai et al., 2006). Tumours with reduced NIS activity are therefore generally associated with a poor prognosis. An understanding of the factors repressing NIS activity is thus important for improvement of radioiodine delivery to tumours that fail to uptake radioiodine effectively. Furthermore, such advances might have profound implications for the treatment of breast cancer and other nonthyroidal cancers currently being assessed for potential NIS-mediated radioiodine therapy (Boelaert and Franklyn, 2003).

Pituitary tumor transforming gene (*PTTG*) produces a multifunctional protein, that can transactivate basic fibroblast growth factor (FGF-2), an action that is dependent on PTTG-binding factor (PBF) (Chien and Pei, 2000). PBF, also known as PTTG1IP or c21orf3 (Yaspo et al., 1998), promotes transformation in vitro and is tumourigenic in vivo (Stratford et al., 2005). However, its exact function is not known. Heaney and colleagues initially implicated PTTG and FGF-2 in the downregulation of NIS activity (Heaney et al., 2001). Subsequently, an association between PTTG overexpression in differentiated thyroid cancers and decreased radioiodine uptake during follow-up was reported (Saez et al., 2006). PTTG and PBF are both overexpressed in thyroid and other tumours, and we have shown that high expression of each gene in thyroid cancer is independently associated with aggressive tumour behaviour (Boelaert et al., 2003; Stratford et al., 2005). We recently examined the influence of PTTG and PBF on human NIS activity and found that both inhibited iodide uptake and NIS expression in vitro. Furthermore, we used promoter studies to map the elements responsible for this transcriptional repression (Boelaert et al., 2007).

Although PTTG and PBF repressed iodide uptake in primary thyroid cells by ~70%, inhibition of NIS promoter activity approximated 40-50% (Boelaert et al., 2007). This led us to speculate that other mechanisms might exist by which PTTG and PBF regulate NIS in thyroid cells. Our data implied that PTTG repression of NIS activity is at least partially dependent on FGF-2, but that an alternative pathway exists for PBF, given that PBF also independently inhibited NIS activity, despite being unable to stimulate FGF-2 (our unpublished data). For active iodide uptake

to occur, NIS must be expressed, targeted and retained at the basolateral plasma membrane of polarised thyroid follicular epithelial cells (Dohan et al., 2001). A number of studies have noted that some thyroid cancers show increased intracellular expression of NIS (Castro et al., 1999b; Dohan et al., 2001; Wapnir et al., 2003). Clearly, altered post-translational regulation of NIS could contribute to a reduction in iodide uptake in thyroid cancers by influencing its subcellular localisation.

In the current investigation, we examined the subcellular localisation of NIS in relation to that of the relatively uncharacterised protein PBF. Our data suggest an entirely novel mechanism by which PBF binds to NIS and alters its subcellular localisation, thereby regulating its ability to uptake iodide.

Results

NIS colocalises with PBF

In fluorescent immunocytochemistry experiments, we determined the localisation of transiently transfected HA-tagged NIS (NIS-HA) and Myc-tagged NIS (NIS-MYC) in monkey kidney COS-7 cells. Both NIS-HA (Fig. 1Ai) and NIS-MYC (Fig. 1Aii) were expressed predominantly at the plasma membrane, but were also apparent in the cytoplasm, where they appeared to reside within intracellular vesicles. To confirm NIS plasma membrane expression, CD8 (cluster of differentiation 8) cDNA was cotransfected with NIS-HA. This encodes a co-receptor involved in antigen recognition, used as a marker for localisation to the plasma membrane (James et al., 2008). A good degree of colocalisation between NIS-HA and CD8 verified the presence of NIS at the cell membrane (Fig. 1B). To determine whether transfected NIS was functional in COS-7 cells, we assessed iodide uptake. NIS-HA transfection resulted in a significant induction of uptake compared with untransfected cells (3425±501 c.p.m. vs 391±95 c.p.m.; $P<0.001$; $n=5$). This confirmed the functionality of exogenous NIS in COS-7 cells, as has been demonstrated previously in a number of publications (Castro et al., 1999a; De la Vieja et al., 2004; De la Vieja et al., 2005; Smanik et al., 1996; Smanik et al., 1997; Van Sande et al., 2003; Zhang et al., 2005). Furthermore, the level of uptake was very similar to that demonstrated by Zhang and colleagues (Zhang et al., 2005).

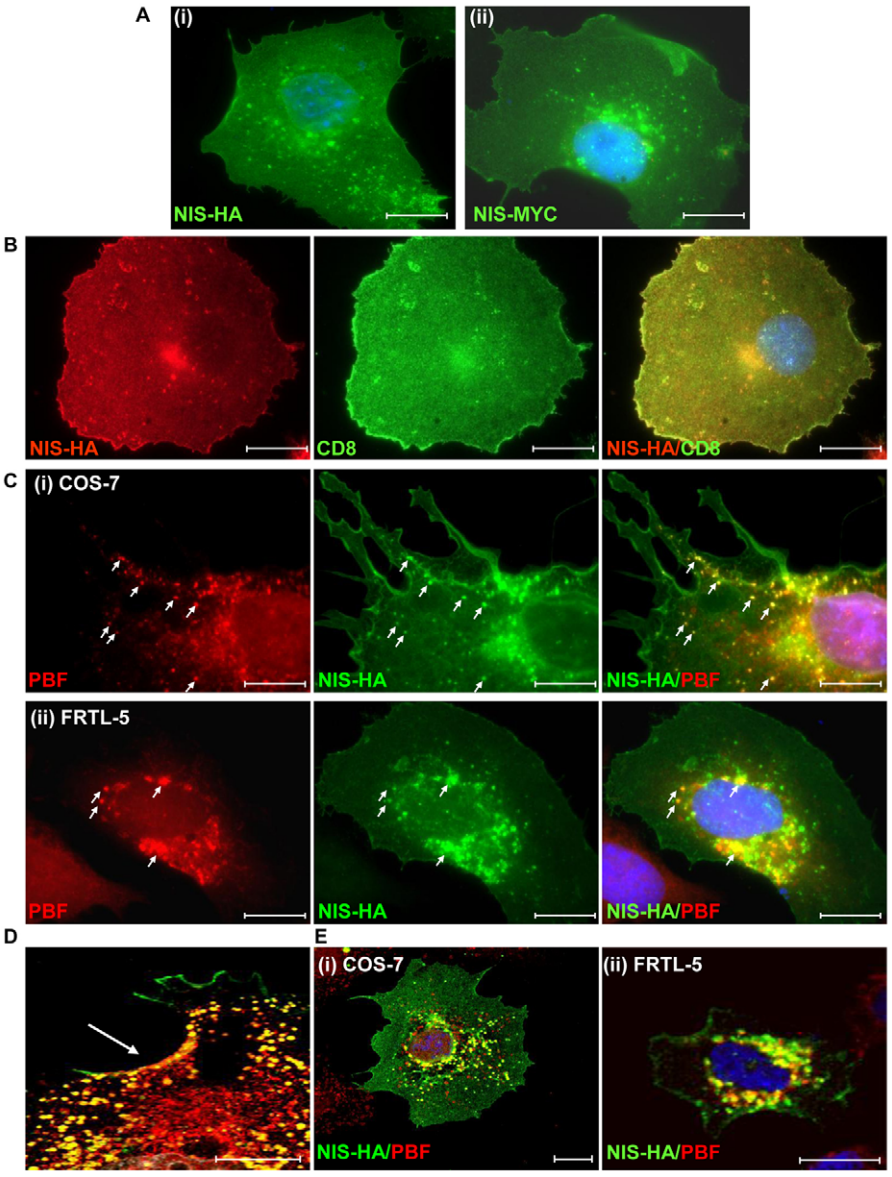

Fig. 1. NIS and PBF localisation in COS-7 and FRTL-5 cells. (A) Following transfection into COS-7 cells and detection by immunofluorescence analysis, NIS-HA (i) and NIS-MYC (ii) demonstrated a similar pattern of expression. Both proteins were located predominantly within the plasma membrane, with partial staining within intracellular vesicles. (B) Coexpression of NIS-HA (red) with the plasma membrane marker CD8 (green) resulted in a high degree of colocalisation as seen in the merged image (yellow). (C) Representative fluorescence immunocytochemistry experiments examining staining of PBF (red) and NIS-HA (green) following transient transfection in COS-7 (i) and FRTL-5 (ii) cells. PBF is predominantly expressed within cytoplasmic vesicles. Merged images demonstrate strong colocalisation between PBF and NIS (yellow) (arrows). (D) Enlarged merged confocal image of PBF (red) and NIS-HA (green) colocalisation (yellow) at the cell surface (arrowed) of a COS-7 cell. (E) Confocal microscopy of NIS and PBF localisation in representative COS-7 and FRTL-5 cells. Colocalisation of PBF and NIS was confirmed by yellow staining in the merged images. Nuclei are visualised in blue with Hoechst 33342 stain in the merged images. Scale bars: 20 μM.

We then assessed the localisation of transiently transfected PBF and NIS-HA in COS-7 cells and rat-thyroid-derived FRTL-5 cells. In COS-7 cells, PBF was expressed at relatively low levels in the nucleus, whereas the majority of PBF protein was concentrated within intracellular vesicles in the cytoplasm (Fig. 1Ci, arrows). Merged images demonstrated strong colocalisation between PBF and NIS, particularly within vesicles. Colocalisation of NIS and PBF was also apparent in the thyroid cell model of FRTL-5 cells (Fig. 1Cii), which demonstrate endogenous NIS expression and iodide uptake (Kogai et al., 1997; Riedel et al., 2001; Schmutzler et al., 1997; Spitzweg et al., 1999). Sites of coincident PBF and NIS staining at the cell membrane were also observed in COS-7 cells (Fig. 1D). Confocal microscopy further delineated the marked overlap between NIS and PBF localisation within COS-7 and FRTL-5 cells (Fig. 1E).

PBF binds NIS in vitro

Having observed strong evidence of PBF and NIS colocalisation in both thyroid and non-thyroidal cell lines, we next investigated whether the two proteins were able to bind in vitro. We performed pull-down assays with in vitro translated L-α-[^{35}S]methionine-labelled NIS and glutathione-S-transferase (GST)-tagged PBF. Binding reactions consistently demonstrated the interaction of labelled NIS with GST-PBF but not with the GST control (Fig. 2A).

Subsequently, coimmunoprecipitation assays were used to assess this interaction in a cellular environment. Following the transient transfection of HA-tagged PBF (PBF-HA) and NIS-MYC into COS-7 cells, NIS was precipitated with an anti-Myc antibody. Coprecipitation of PBF-HA with NIS-MYC was observed by probing with an anti-HA antibody following western blotting (Fig. 2B). By contrast, PBF was not detected in controls in which NIS-MYC and vector-only (VO) or PBF-HA and VO were transfected (Fig. 2B). The reciprocal coimmunoprecipitation was performed using the anti-HA antibody for precipitation of PBF-HA and immunoblotting for NIS-MYC, which similarly resulted in successful coimmunoprecipitation (Fig. 2C, arrows). These results confirm that NIS and PBF not only colocalise, but also interact within these cells.

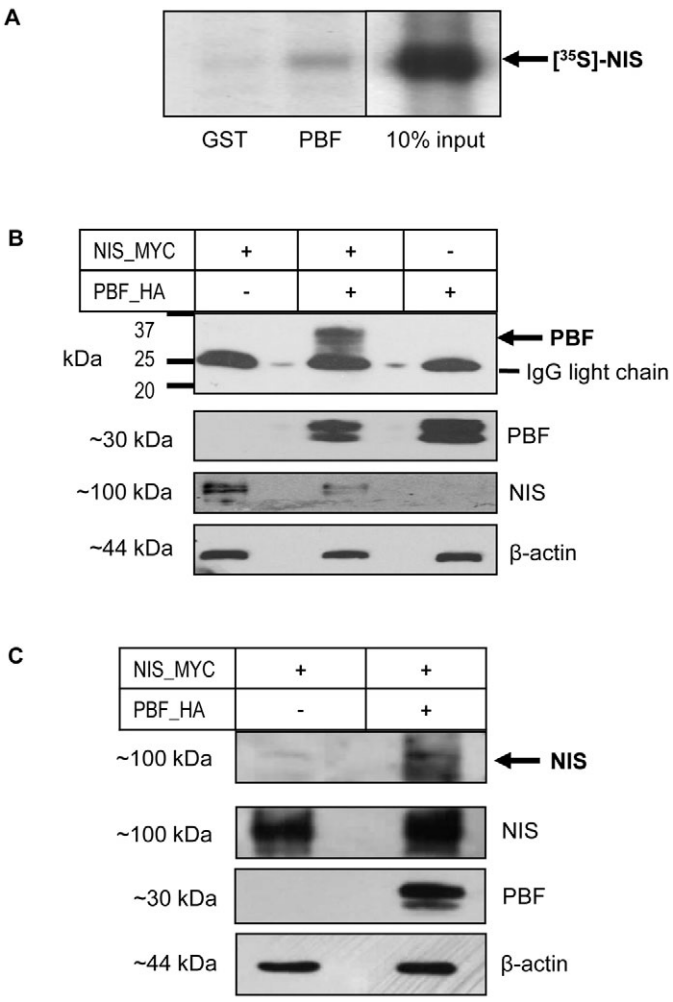

Fig. 2. PBF binds NIS in vitro. (A) Pull-down assay showing in vitro translated L-α- [^{35}S]methionine-labelled NIS binding GST-tagged PBF versus a GST-only control. (B) Coimmunoprecipitation assays in COS-7 cells transfected with NIS-MYC and VO, PBF-HA and VO, or NIS-MYC and PBF-HA. A band corresponding to PBF (arrowed) was observed at approximately 30 kDa when NIS-MYC and PBF-HA were cotransfected but was not present when either NIS-MYC or PBF-HA were transfected with VO. Analysis of total protein cell lysate shown below demonstrates the presence of NIS-MYC or PBF-HA in each sample along with a β-actin loading control. (C) Reciprocal assay following transfection of NIS-MYC and VO or NIS-MYC and PBF-HA. NIS-MYC was coprecipitated along with PBF-HA and detected as a band at approximately 100 kDa (arrow).

PBF alters the subcellular localisation of NIS

In COS-7 cells transfected with NIS-HA (Fig. 3Ai), NIS-HA was localised predominantly within the plasma membrane, with partial staining within intracellular vesicles. Endogenous PBF was mainly localised within cytoplasmic vesicles, with some apparent nuclear staining. However, when PBF was cotransfected with NIS-HA, there was an increase of NIS staining within intracellular vesicles and a concomitant reduction in membrane staining (Fig. 3Aii). Given that PBF and NIS bound each other in pull-down and coimmunoprecipitation assays, we therefore investigated by quantitative means whether PBF overexpression was associated with diminished NIS localisation at the cell membrane, where NIS is functional. We transfected COS-7 cells with NIS-HA, and either VO control or human PBF. Cell surface biotinylation assays confirmed a reduction in plasma membrane expression of NIS following PBF transfection compared with VO treatment (32±9% reduction; P=0.018; n=3) (Fig. 3Bi). By contrast, total NIS-HA expression was not significantly altered by PBF overexpression compared with VO (2±3% reduction; P=0.529; n=3) (Fig. 3Bii). Hence, when PBF expression is increased in COS-7 cells, plasma membrane expression of NIS decreases.

Colocalisation of PBF, NIS and CD63

Detailed examination of our patterns of intracellular staining for PBF and NIS (as shown in Figs 1 and 3) raised the possibility that these proteins were localised to late endosomes. To assess this hypothesis, we examined expression of the late endosome marker CD63, a member of the tetraspanin family commonly associated with clathrin-dependent trafficking. We transfected COS-7 cells with NIS-HA, and examined its relationship to endogenous CD63. Merged images revealed a high degree of colocalisation (Fig. 4Ai). We performed analogous studies with PBF and CD63, which revealed similar patterns of colocalisation within late endosomes (Fig. 4Aii). Finally, we assessed staining of caveolin-1, the main constituent of caveolae which acts as a regulator of caveolae-

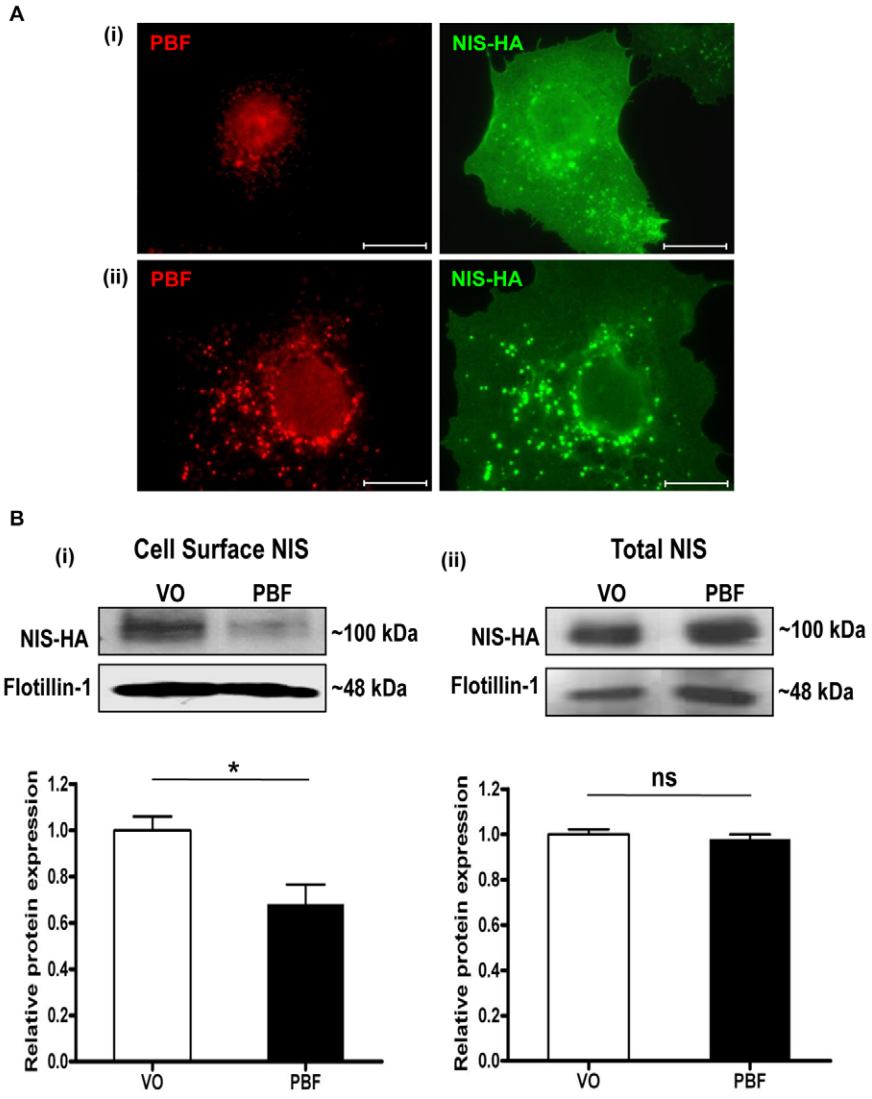

Fig. 3. PBF alters the subcellular localisation of NIS. (A) (i) Immunofluorescent detection of NIS-HA and endogenous PBF in cells transfected with NIS-HA and VO control. (ii) PBF overexpression is associated with an increase in NIS staining within intracellular vesicles. Scale bars: 20 μM. (B) Cell-surface biotinylation assay in COS-7 cells transfected with a VO control or with human PBF. (i) Representative immunoblot analysis of surface-biotinylated polypeptides precipitated with streptavidin-agarose beads and probed with anti-HA antibody, which revealed HA-tagged human NIS detection at around 100 kDa. Flotillin-1 was used as a marker of membrane protein expression to determine loading between samples. (ii) Total NIS-HA protein expression. Graphs indicate mean differences in cell-surface and total expression of NIS (n=3 separate scanning densitometry experiments were performed). *P<0.05; ns, not significant.

dependent lipid trafficking and endocytosis. When we examined caveolin-1 localisation in COS-7 cells, we found no overlap with either PBF or NIS expression (Fig. 4Aiii). Confocal microscopy confirmed the strong colocalisation apparent between NIS, PBF and CD63 (Fig. 4Bi), and the lack of association between NIS, PBF and caveolin-1 (Fig. 4Bii). Thus, NIS and PBF colocalise with CD63 but not with caveolin-1, suggesting that clathrin-dependent rather than caveolin-dependent endocytosis is responsible for the internalisation of these proteins.

Localisation of PBF deletion mutants

To investigate the relationship between PBF and NIS further, we constructed three deletion mutants of PBF. The PBF protein is extremely poorly characterised, and has no significant homology to other human proteins. A putative signal peptide lies at the N-terminus, followed by a putative PSI domain (a cysteine-rich region common to plexins, semaphorins and integrins) between amino acids 39 and 92, and a potential transmembrane region between residues 95 and 122 (Fig. 5A). At the C-terminus, predicted nuclear localisation and tyrosine-based sorting signals lie between amino acids 149 and 174. Given the lack of functional data on PBF, we therefore created three HA-tagged deletion mutants. Mutant 1 (M1) lacked the C-terminal 30 amino acids (149-180), which have previously been shown to mediate its binding to PTTG (Chien and Pei, 2000). Mutant 2 (M2) had a deletion of residues 29-93, which encompassed part of the signal peptide and the putative PSI domain, and Mutant 3 (M3) lacked amino acids 94-149, containing the potential transmembrane domain (Fig. 5A).

The localisation of each of the mutants in comparison to HA-tagged wild-type (WT) PBF was initially assessed following transient transfection into COS-7 cells. Confocal images once more identified WT PBF predominantly within intracellular vesicles (Fig. 5Bi). By contrast, M1 was located almost exclusively in the plasma membrane. M2 and M3 appeared to be expressed predominantly in the endoplasmic reticulum (Fig. 5Bi). Strong colocalisation of M1 was observed with the CD8 plasma membrane marker whereas no significant colocalisation was seen with WT PBF, M2 or M3 (Fig. 5Bii). Similarly, M2 and M3 demonstrated a high degree of colocalisation with endogenous protein disulphide isomerase (PDI), a marker for the endoplasmic reticulum, whereas WT PBF and M1 showed minimal costaining

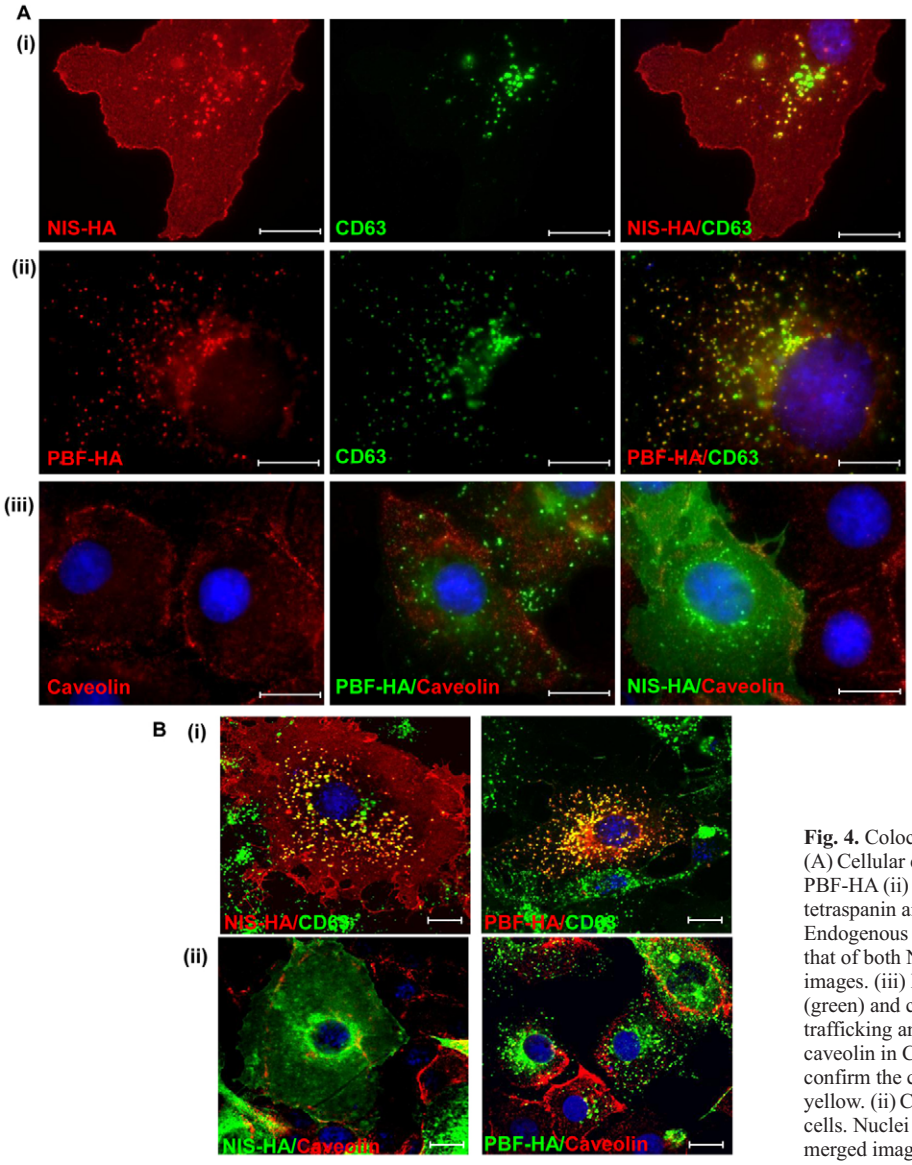

Fig. 4. Colocalisation studies of NIS, CD63, PBF and caveolin. (A) Cellular expression of transiently transfected NIS-HA (i) and PBF-HA (ii) (both red) with endogenous CD63 (green), a tetraspanin and a marker of late endosomes, in COS-7 cells. Endogenous CD63 staining in late endosomes is coincident with that of both NIS and PBF, as indicated by yellow staining in merged images. (iii) Relationship between PBF-HA (green), NIS-HA (green) and caveolin-1 (red), a marker of caveolae-dependent lipid trafficking and endocytosis. Neither PBF nor NIS colocalises with caveolin in COS-7 cells. (B) (i) Confocal microscopy was used to confirm the colocalisation of NIS and PBF with CD63, shown in yellow. (ii) Confocal images of NIS, PBF and caveolin in COS-7 cells. Nuclei are visualised in blue with Hoechst 33342 stain in the merged images. Scale bars: 20 µM.

(Fig. 5Biii). Notably, unlike WT PBF, none of the mutants colocalised with CD63 (Fig. 5Biv), strongly suggesting they were not expressed within late endosomes.

PBF, NIS and iodide uptake

We next examined the colocalisation of WT and mutant PBF with NIS. HA-tagged WT PBF and the three mutants were each transiently transfected into COS-7 cells along with NIS-MYC. Localisation of WT PBF and the mutants (Fig. 6Ai) was as described previously (Fig. 5Ai). Whilst NIS showed intense staining within intracellular vesicles in the presence of WT PBF, it remained predominantly membranous when coexpressed with each of the mutants (Fig. 6Aii). Merged images demonstrated again WT PBF colocalisation with NIS in intracellular vesicles (Fig. 6Aiii). M1 showed strong colocalisation with NIS at the cell membrane, but not intracellularly, whereas M2 and M3 failed to significantly colocalise with NIS (Fig. 6Aiii).

Finally, we investigated the effect of altered PBF localisation upon endogenous NIS activity. We therefore used FRTL-5 thyroid cells, which show significant endogenous iodide uptake (Kogai et al., 1997; Riedel et al., 2001; Schmutzler et al., 1997; Spitzweg et al., 1999) and show colocalisation of NIS and PBF (Fig. 1). We first confirmed that FRTL-5 cells express endogenous PBF (supplementary material Fig. S1). Subsequently, we manipulated PBF expression through transient transfection of WT and mutant PBF constructs. Immunofluorescence analyses established that the localisation of WT and mutant PBF was consistent with that observed in COS-7 cells (Fig. 6B): WT PBF was apparent in intracellular vesicles, M1 localised to the membrane, and M2 and M3 localised to the ER. Iodide-uptake experiments were then performed. Data from FRTL-5 cells were normalised to iodide uptake in VO controls, which gave a mean count of 1029 c.p.m. after incubation with 0.05 µCi ^{125}I for 1 hour. WT PBF repressed iodide uptake into FRTL-5 cells by 39.4±5% (P<0.001; n=10) compared with VO control (Fig. 6C). By contrast, all three deletion mutants of PBF, which do not localise within intracellular vesicles in COS-7 or FRTL-5 cells, lost the ability to inhibit NIS activity (M1, 104.3±13%; M2, 89.2±11%; M3, 109.6±14%; P=NS compared with VO control) (Fig. 6C).

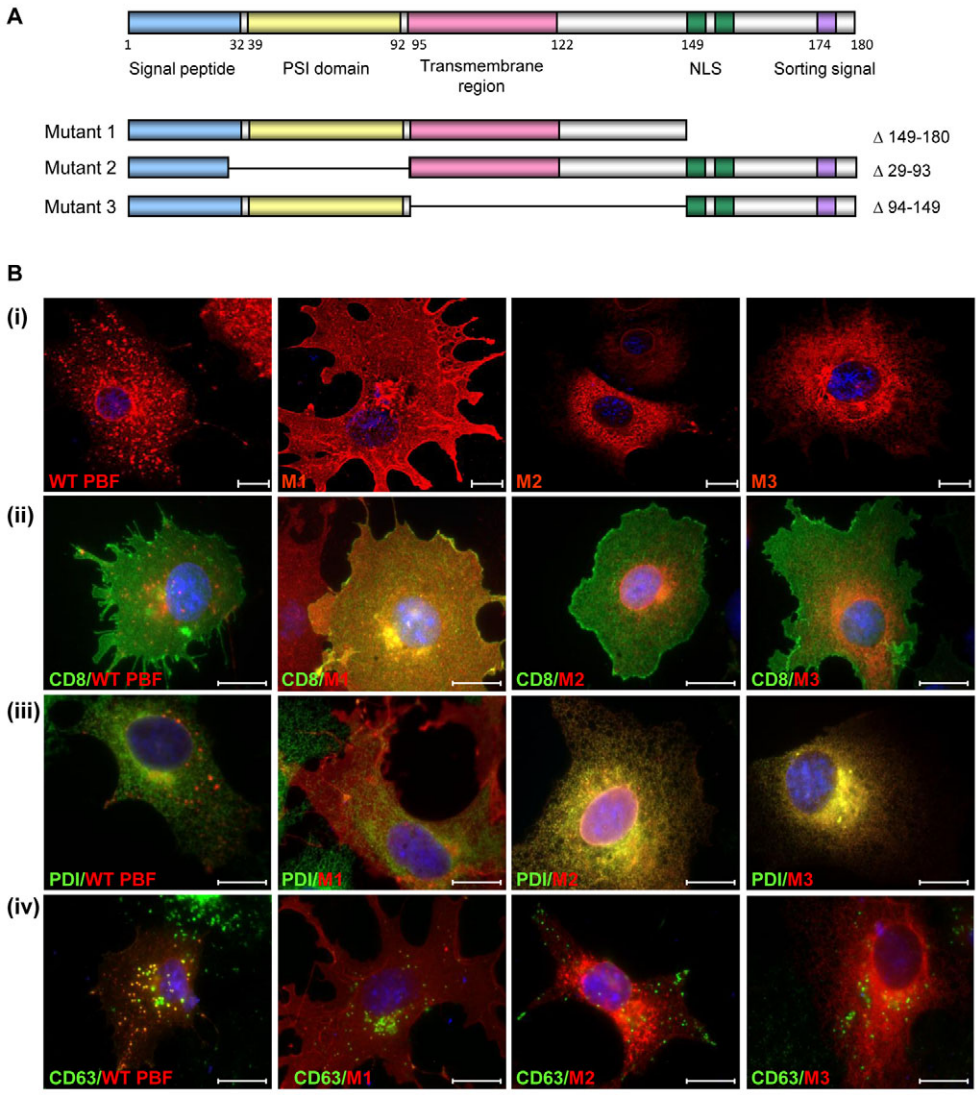

Fig. 5. Localisation of PBF deletion mutants. (A) Putative functional domains of WT PBF, as well as three deletion mutants M1, M2 and M3. NLS, nuclear localisation signal. Site-directed mutagenesis was used to delete the C-terminal 30 amino acids (149-180) for M1. M2 had a deletion of amino acids 29-93 and M3 lacked amino acids 94-149, containing the potential transmembrane domain. (B) (i) Confocal images demonstrating the localisation of each of the mutant PBF proteins compared with wild-type PBF in COS-7 cells. M1 is predominantly in the cell membrane whereas M2 and M3 appear to be in the endoplasmic reticulum. (ii) Coexpression of CD8 confirmed the presence of M1 in the plasma membrane. (iii) Endogenous PDI staining verified endoplasmic reticulum expression of M2 and M3. (iv) Intracellular expression of WT and mutated PBF with CD63 in COS-7 cells. Unlike the WT, none of the mutants show significant colocalisation with CD63. Scale bars: 20 μM.

Taken together, these data support the hypothesis that PBF and NIS colocalise within late endosomes, and that upregulation of PBF redistributes NIS away from the plasma membrane into these organelles, a mechanism that significantly represses cellular iodide uptake.

Discussion

The regulation of membrane transport proteins is an intricate process, and NIS regulation is characteristically complex. As an integral membrane glycoprotein which mediates active iodide transport into thyroid cells, NIS acts as the crucial first step in thyroid hormone biosynthesis (Boelaert and Franklyn, 2003; Dohan et al., 2003). The ability of the thyroid to accumulate iodide has provided an effective means for therapeutic doses of radioiodine to target and destroy iodide-transporting differentiated thyroid cancers and their metastases. However, most thyroid tumours exhibit reduced iodide uptake and a number of mRNA (Lazar et al., 1999; Park et al., 2000; Ringel et al., 2001; Ryu et al., 1999; Smanik et al., 1997; Ward et al., 2003) and protein (Caillou et al., 1998; Faggiano et al., 2007; Gerard et al., 2003; Jhiang et al., 1998; Trouttet-Masson et al., 2004) studies have reported decreased NIS expression in thyroid cancers, suggesting that the reduction in iodide uptake is due to a transcriptional effect.

By contrast, several other studies have shown either normal, or even increased levels of NIS mRNA (Arturi et al., 1998; Luciani et al., 2003; Saito et al., 1998; Tanaka et al., 2000) or protein (Dohan et al., 2001; Saito et al., 1998; Wapnir et al., 2003) expression in thyroid cancer. However, immunohistochemical analyses have detected NIS protein that was not located predominantly in the basolateral membrane, as found in normal thyroid tissue, but was principally in the cytoplasm (Castro et al., 1999b; Dohan et al., 2001; Wapnir et al., 2003). This suggests that the reduction in iodide uptake in thyroid cancer is at least partially attributable to altered NIS trafficking and subcellular localisation, which might therefore be more relevant than expression levels per se. Understanding the factors regulating NIS localisation and activity in thyroid tumours is thus important in improving radioiodine delivery to those tumours that fail to uptake radioiodine effectively.

At present, little is known about the regulation of NIS trafficking. In addition to stimulating cAMP-mediated NIS expression, TSH is also required for post-translational regulation of NIS (Riedel et al., 2001). Studies using FRTL-5 cells have

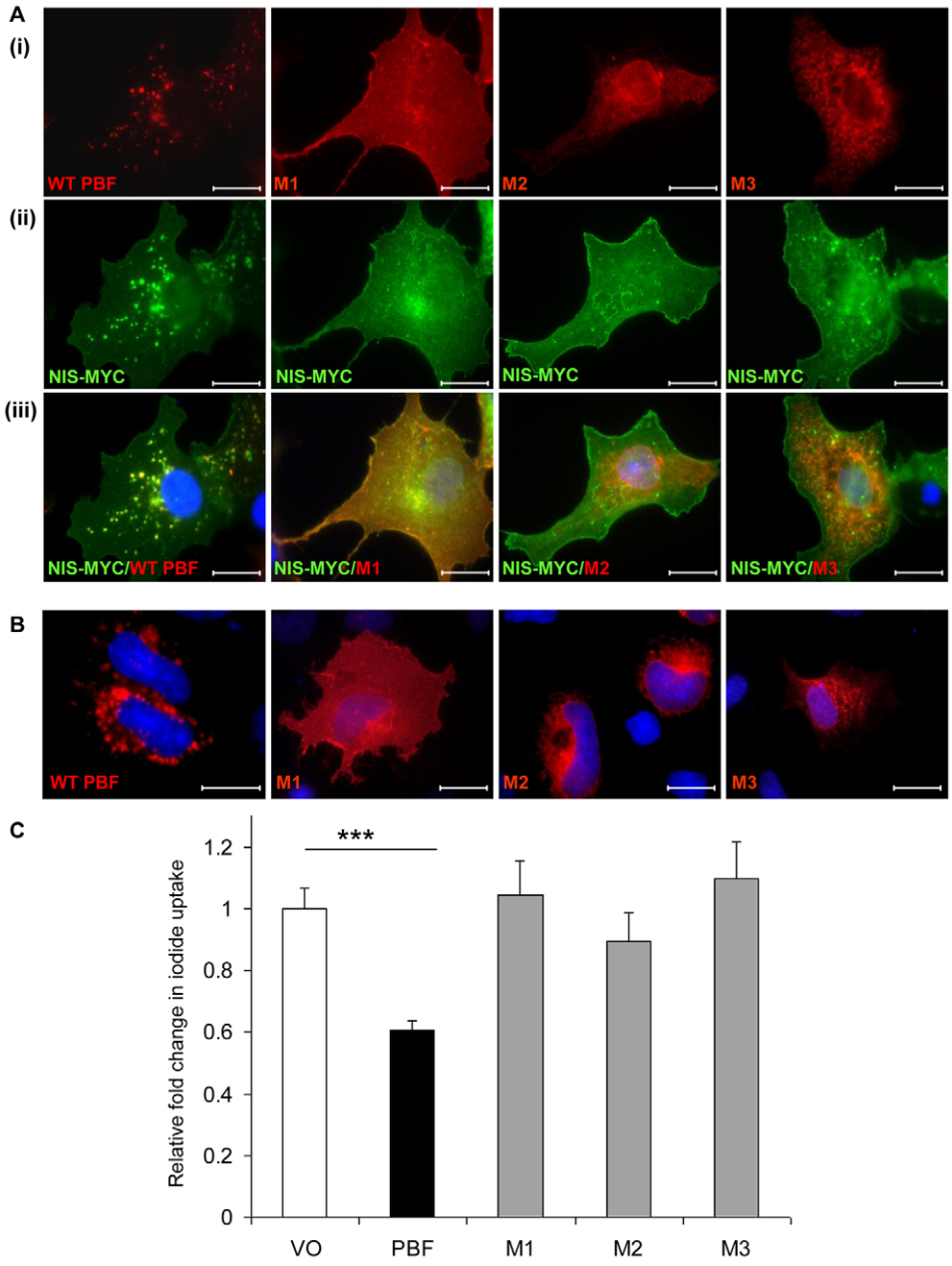

Fig. 6. The effect of PBF on NIS function. (A) Examination of the subcellular localisation of WT and mutated HA-tagged PBF in COS-7 cells (i), Myc-tagged NIS (ii) and colocalisation (iii). WT PBF predominantly colocalises with NIS within late endosomes. M1 colocalises with NIS at the cell membrane, whereas M2 and M3 fail to show any significant colocalisation with NIS. (B) Confocal images demonstrating the localisation of WT and mutant PBF in FRTL-5 cells. Scale bars: 20 µM. (C) Iodide-uptake studies in rat thyroid FRTL-5 cells transfected with WT PBF and mutants M1, M2 and M3. Graph shows c.p.m. values normalised to that of the VO control. ***P<0.001.

alluded to a mechanism by which NIS is located in the plasma membrane of thyroid cells in the presence of TSH, but is redistributed into intracellular vesicles upon TSH withdrawal. TSH is thus required for either the targeting of NIS to the plasma membrane or its retention there (Kaminsky et al., 1994; Kogai et al., 1997; Riedel et al., 2001). NIS is a phosphoprotein that has demonstrated different patterns of phosphorylation in FRTL-5 cells maintained in the presence or absence of TSH (Riedel et al., 2001). Phosphorylation of the C-terminus has been proposed to influence plasma membrane targeting of NIS (Dohan et al., 2005). However, although a number of phosphorylated residues have been confirmed, none has been shown to affect NIS cell membrane trafficking (Vadysirisack et al., 2007). A recent study assessing NIS regulation in breast cancer demonstrated that phosphatidylinositol-3 kinase (PI3K) activation interferes with cell-surface trafficking and function of all-*trans* retinoic acid and hydrocortisone (tRAH)-induced endogenous NIS, as well as transiently expressed exogenous NIS, in the MCF-7 human mammary carcinoma cell line (Knostman et al., 2007).

In the present study, we have assessed a potential role for PBF in the post-translational regulation of NIS activity, given its ability to repress iodide uptake. Although NIS was expressed at the cell surface, it was also present in intracellular vesicles reminiscent of those previously described (Kaminsky et al., 1994; Riedel et al., 2001). Similarly to NIS, PBF is also a predicted integral membrane glycoprotein (Yaspo et al., 1998). PBF was predominantly located in similar vesicular structures to NIS, and was also apparent at the plasma membrane. Our description of PBF localisation differs from a previous report (Chien and Pei, 2000), which did not describe vesicular staining. In common with this earlier study, we did observe a degree of nuclear localisation. However, our current and previous (Stratford et al., 2005) investigations into PBF suggest that the

protein is highly expressed in the cytoplasm. Validation of our antibody assessment of PBF localisation within intracellular vesicles is provided in supplementary material Fig. S2.

Given that PBF and NIS demonstrated strong colocalisation within such vesicles, we investigated whether PBF could bind NIS in vitro using pull-down and coimmunoprecipitation assays. GST-tagged PBF consistently pulled down [^{35}S]-labelled NIS, and PBF-HA coprecipitated with NIS-MYC in COS-7 cells, indicating that the proteins can interact. Critically, increased expression of PBF in COS-7 cells was accompanied by reduced plasma membrane expression of NIS, as determined through cell-surface biotinylation assays. This was in agreement with our immunofluorescent microscopy studies, which suggested an increased vesicular localisation of NIS in response to augmented PBF expression. Thus, NIS and PBF colocalise, bind each other, and PBF is able to alter the subcellular localisation of NIS. The physiological relevance of this phenomenon is a direct one. PBF is overexpressed in differentiated thyroid cancers (Stratford et al., 2005), which as a consequence would be expected to have a lower ability to uptake iodide, and hence a poorer response to radioiodine treatment. To test this hypothesis, it would therefore be interesting in future studies to assess PBF and NIS expression and localisation in a large series of differentiated thyroid tumours and to relate this to clinical outcome.

To investigate the vesicles in which PBF and NIS colocalised, we assessed CD63 staining. CD63 is a tetraspanin involved in protein trafficking and is located in a number of intracellular structures, including late endosomes and lysosomes, in addition to the cell membrane. At the C-terminus, CD63 has a YxxΦ motif, a tyrosine-based sorting signal, which has been shown to interact with adaptor protein (AP) complexes, thereby linking trafficking of CD63 to clathrin-dependent pathways (Berditchevski and Odintsova, 2007). We determined that both PBF and NIS showed a strong degree of colocalisation with CD63. Based on these findings, the presence of a YxxΦ motif at the C-terminus of PBF, and the fact that neither PBF nor NIS colocalises with caveolin-1, a regulator of caveolae-dependent lipid trafficking and endocytosis, we propose that PBF and NIS are indeed enriched within late endosomes, and use a clathrin-pit-mediated mechanism of internalisation.

NIS has a long half-life, estimated at 3-5 days (Riedel et al., 2001), and a hence a mechanism of post-translational regulation of activity would allow cells to respond to, and regulate their need for, iodide uptake over a much shorter timeframe. Indeed, we observed significant internalisation of NIS within 48 hours of PBF transfection. Membrane vesicles, which have been reported to contain NIS, were enriched for plasma membrane content, suggesting an endocytosis-mediated pathway of NIS regulation (Kaminsky et al., 1994). Our data shed new light on this mechanism, in that we have identified a protein that appears to significantly modulate this process.

A final strand of supporting evidence that supports our hypothesis came from iodide uptake studies in rat thyroid FRTL-5 cells. The protein structure of PBF is very poorly understood, and hence we constructed three PBF mutants, lacking the C-terminal YxxΦ motif (M1), a putative signal peptide and the putative PSI domain (M2), and the potential transmembrane region (M3). All three mutants lost vesicular enrichment, and failed to colocalise significantly with CD63 or with NIS. Iodide-uptake assays in FRTL-5 cells complemented our previous finding in human primary thyroid cells that PBF represses iodide uptake (Boelaert et al., 2007). The magnitude of effect was ~40%, which contrasts with our conservative estimate of transfection efficiency of 15-25%. This suggests either that we might be underestimating transfection efficiency by focusing only on strongly fluorescent GFP expression, or that other mechanisms exist (e.g. paracrine regulation of surrounding cell function). However, this is beyond the scope of the present investigation. In contrast to WT PBF, all three mutants failed to significantly influence iodide uptake compared with the control. This suggests that PBF requires endosomal entry to modulate NIS localisation and function. When the protein structure of PBF is resolved, it will be important to perform more subtle mutation analysis, investigating point mutations targeting specific and characterised domains, allowing us to elucidate this mechanism further.

One caveat to these studies is that because it is not known what regulates PBF, we are unable to manipulate its endogenous expression, and hence have used a largely exogenous system in COS-7 cells. Furthermore, immunofluorescence for native NIS expression is technically challenging in FRTL-5 cells. For this reason, most studies of NIS in the literature have focused on COS-7 cell manipulations. Indeed, in our hands, NIS was entirely functional in COS-7 cells, yielding extremely similar iodide uptake to that previously reported by Zhang and co-workers (Zhang et al., 2005).

Overall, the clinical relevance of PBF repression of NIS activity relates to its likely influence upon the efficacy of radioiodine therapy. The ability of the thyroid to accumulate iodide provides the basis for radioiodine ablation of iodide-transporting differentiated thyroid cancers and their metastases. Taken together, we propose that through downregulation of NIS via alteration of its subcellular localisation, increased PBF could fundamentally influence the prognosis of differentiated thyroid cancers, at least in part, through affecting their sensitivity to ablative radioiodine therapy.

Materials and Methods

Plasmids and mutagenesis

The full-length human NIS cDNA was kindly provided by John Morris (Mayo Graduate School of Medicine, Mayo Clinic, Rochester, MN) (Castro et al., 1999a). This was inserted into the *Eco*RI and *Xho*I restriction sites of the pcDNA3.1+ vector (Invitrogen, Carlsbad, CA) and simultaneously tagged on the 3′ end with either the HA epitope using the forward primer, 5′-GCC GAA TTC CCA CCA TGG AGG CCG TGG AGA CC-3′ and reverse primer, 5′-CGG CTC GAG TCA AGC GTA GTC TGG GAC GTC GTA TGG GTA GAG GTT TGT CTC CTG CTG G-3′ (NIS-HA), or the Myc epitope using the same forward primer, and the reverse primer, 5′-CGG CTC GAG TCA GGA TCC CAG GTC CTC CTC GGA AAT CAG CTT CTG CTC AAG GTT TGT CTC CTG CTG G-3′ (NIS-MYC).

Plasmids containing the full-length PBF cDNA with (PBF-HA) and without (PBF) a HA tag have previously been described (Stratford et al., 2005). Three deletion mutants of PBF were created by mutating the PBF-HA plasmid using the QuikChange Site-Directed Mutagenesis Kit (Stratagene, Cambridge, UK) using the following primers: M1_forward, 5′-GAGAGGCGGATACGGCAGGAGGAATACCCATAC-GACGTCCCAGACTAC-3′; M1_reverse, 5′-GTAGTCTGGGACGTCGTATG-GGTATTCCTCCTGCCGTATCCGCCTCTC-3′; M2_forward, 5′-CTCCTGCT-GCTCATCCCGAACTTTGAGGCGCTGATC-3′; M2_reverse, 5′-GATCAGCGC-CTCAAAGTTCGGGATGAGCAGCAGGAG-3′; M3_forward, 5′-GCTGGG-GAGTTTGTTGGGTGCGGAGAGCAGAGATGAAGAC-3′; M3_reverse, 5′-GTCTTCATCTCTGCTCTCCGCACCCAACAAACTCCCCAGC-3′.

Additionally, cDNA encoding CD8 was kindly provided by Barbara Reaves (Department of Biology and Biochemistry, University of Bath, UK) (James et al., 2008).

Cell lines and transient transfection

FRTL-5 cells are a nontransformed rat thyroid cell line, which were grown in modified Coon's F-12 medium as described (Ambesi-Impiombato et al., 1980) (Gibco, Paisley, Scotland). The medium was supplemented with TSH (300 mU/l), insulin (100 μg/l), penicillin (10^5 U/l), streptomycin (100 mg/l) and 5% fetal bovine serum (FBS).

The COS-7 African Green monkey kidney epithelial cell line was maintained in DMEM medium (Gibco) supplemented with 10% FBS, penicillin (10^5 U/l) and

streptomycin (100 mg/l). The H1299 non-small cell lung carcinoma cell line was maintained in RPMI 1640 medium (Gibco) supplemented with 10% FBS, sodium pyruvate (1 mM), glucose (3.5 g/l), HEPES (10 mM), penicillin (10^5 U/l) and streptomycin (100 mg/l).

Cells were transfected using Fugene 6 reagent (Roche, Indianapolis, IN) following the manufacturer's instructions at a 3:1 reagent:DNA ratio. For iodide-uptake assays, immunofluorescence staining, coimmunoprecipitation assays and cell-surface biotinylation assays, cells were seeded in 24-well plates, six-well plates with sterile coverslips, T25 flasks or T75 flasks, respectively, and transfected with 0.5 μg, 2 μg, 5 μg or 15 μg DNA after 24 hours.

The pMax-GFP plasmid (Amaxa, Cologne, Germany) was used to determine the transfection efficiency of FRTL-5 cells. Routinely, transfection efficiency was between 15 and 25% in FRTL-5 cells (see supplementary material Fig. S3).

Immunofluorescence staining

Medium was removed 48 hours after transfection, and cells were washed with phosphate-buffered saline (PBS). Cells were fixed for 20 minutes at room temperature in 0.1 M phosphate buffer (pH 7.4) containing 2% paraformaldehyde, 2% glucose and 0.02% sodium azide. After rinsing twice in PBS, cells were permeabilised in 100% chilled methanol for 10 minutes and then blocked with 10% newborn calf serum (NCS) in PBS for 30 minutes at room temperature.

Incubation with primary antibody was performed at room temperature for 1 hour in 1% BSA. The following antibodies were used: rabbit polyclonal anti-HA (Y-11) antibody (Santa Cruz Biotechnology, Santa Cruz, CA), mouse monoclonal anti-HA.11 antibody (Covance Research Products, Emeryville, CA), rabbit polyclonal anti-PBF antibody (made by Eurogentec, Seraing, Belgium) for our laboratory using the full-length PBF protein as an epitope), mouse monoclonal anti-human CD8 antibody (UCHT4; Ancell Corporation, Bayport, MN), mouse monoclonal anti-protein disulphide isomerase (PDI) antibody (Stressgen, San Diego, CA), mouse monoclonal anti-CD63 antibody (kindly provided by Fedor Berditchevski, School of Cancer Sciences, University of Birmingham, Birmingham, UK), mouse monoclonal anti-Myc-Tag (9B11) antibody (Cell Signaling Technology, Danvers, MA), and rabbit anti-caveolin (kindly provided by Melissa Westwood, University of Manchester, UK).

Cells were rinsed three times with PBS before a further 1 hour incubation with the secondary antibodies, Alexa-Fluor 488-conjugated goat anti-mouse IgG and Alexa-Fluor-594-conjugated goat anti-rabbit IgG (Invitrogen) at 1:250 in 1% BSA, with 1% NCS and Hoechst 33342 stain for nuclei (1:1000). Finally, cells were rinsed with PBS three times and coverslips mounted onto slides using Dako Fluorescent Mounting Solution (Dako, Glostrup, Denmark).

Conventional microscopy was performed using a 100× objective on a Zeiss Axioplan fluorescent microscope (Zeiss, Germany). A Zeiss confocal LSM 510 microscope with a 63× objective was used to perform confocal microscopy.

In vitro transcription: translation and glutathione-S-transferase (GST) pull-down assays

The TNT Coupled Reticulocyte Lysate System (Promega, Madison, WI) was used to express protein from the NIS-HA plasmid following the manufacturer's instructions. The following reaction components were assembled: 50 μl TNT Rabbit Reticulocyte Lysate, 4 μl TNT Reaction Buffer, 2 μl amino acid mixture (minus methionine; 1 mM), 4 μl L-α-[^{35}S]methionine, 1 μl RNasin Ribonuclease Inhibitor (40 U/μl), 2 μg plasmid DNA, 2 μl TNT RNA Polymerase (T7) and 29 μl nuclease-free water. The reaction was incubated at 30°C for 2 hours.

PBF was expressed as a fusion protein with glutathione-S-transferase (GST) from a pGEX plasmid (Amersham) as described previously (Turnell et al., 2000). Along with a GST-only control, 20 μg GST-tagged PBF protein were combined with 10 μl L-α-[^{35}S]methionine-labelled NIS protein and incubated for 1 hour on ice. Following the addition of 400 μl low-salt buffer (50 mM Tris-HCl pH 7.4, 150 mM NaCl, 1% NP-40), 40 μl of packed glutathione agarose beads were added to each reaction, which was subsequently incubated with end-over-end mixing using a rotator for 90 minutes at 4°C. After washing with the low-salt buffer, bound GST-PBF protein was eluted with 40 μl of 25 mM glutathione in 50 mM Tris-HCl, pH 8, on ice for 1 hour. The protein samples were then analysed by SDS-PAGE, using a 12% acrylamide gel, along with 1 μl L-α-[^{35}S]methionine-labelled NIS protein in 20 μl Laemmli sample buffer with 5% (v/v) β-mercaptoethanol, used as a control demonstrating 10% input. Following electrophoresis, the gel was fixed and stained. The gel was then immersed in Amplify Fluorographic Reagent (Amersham Biosciences, Little Chalfont, Buckinghamshire, UK) to increase the sensitivity of signal detection, dried at 65°C for 2 hours and, finally exposed to autoradiographic film at –20°C.

Coimmunoprecipitation assays

COS-7 cells in T25 flasks were transiently transfected with either NIS-MYC and pCI-neo (VO), PBF-HA and pcDNA3.1+ (VO) or NIS-MYC and PBF-HA. Cells were harvested in 500 μl RIPA buffer (50 mM Tris-HCl, pH 7.4, 150 mM NaCl, 1% v/v Igepal CA-630, 6 mM sodium deoxycholate, 1 mM EDTA) containing protease inhibitor cocktail (Sigma, Poole, Dorset, UK). After a brief sonication step, cell lysates were centrifuged at 15,700 ***g*** for 20 minutes and transferred to a clean Eppendorf. Each lysate was incubated with 12.5 μl mouse monoclonal anti-Myc-Tag (9B11) antibody at 4°C overnight with end-over-end rotation. Following the addition of 25 μl packed beads prepared from Protein-G-Sepharose 4 Fast Flow (Amersham), the samples were incubated for a further 2 hours at 4°C with end-over-end rotation. An antibody-only control consisting of 12.5 μl anti-Myc antibody and 25 μl packed beads in 500 μl RIPA buffer was also established. Protein-G-Sepharose beads were centrifuged and, following the removal of any unbound protein, washed four times with 500 μl RIPA buffer. Bound protein was eluted in 50 μl Laemmli Sample Buffer (Bio-Rad Laboratories, Hercules, CA) containing 5% (v/v) β-mercaptoethanol and 1% (w/v) SDS at 37°C for 30 minutes.

Proteins were separated by SDS-PAGE using a 15% acrylamide gel and transferred to polyvinylidene difluoride membrane. The membrane was blocked with 5% milk in TBS containing 0.025% Tween 80 and PBF-HA protein was probed with rabbit polyclonal anti-HA (Y-11) antibody at a concentration of 1:1000 in blocking buffer. Following incubation with Protein-G-HRP (Bio-Rad), the antigen-antibody complexes were detected using the ECL-Plus chemiluminescence detection system (Amersham). Total protein cell lysate (20 μg) taken before the coimmunoprecipitation steps was also separated by SDS-PAGE using 7.5% and 15% acrylamide gels to probe for NIS-MYC and PBF-HA, respectively. PBF-HA was probed in the same way as the coimmunoprecipitation samples and NIS-MYC detected with mouse anti-Myc antibody at a concentration of 1:1000 with 650 ng/ml HRP-conjugated polyclonal rabbit anti-mouse immunoglobulins (Dako) as secondary antibody. β-actin expression was assessed as a loading control for each protein.

The reciprocal experiment was performed in the same way by precipitating PBF-HA with 12.5 μl mouse monoclonal anti-HA.11 antibody (Covance Research Products) and probing for coimmunoprecipitated NIS-MYC with mouse monoclonal anti-Myc-Tag (9B11) antibody.

Cell-surface biotinylation

In each of four T75 flasks, NIS-HA and either pCI-neo (VO) or PBF plasmids were transiently transfected into COS-7 cells. 48 hours after transfection, the Cell Surface Protein Isolation Kit (Pierce, Rockford, IL) was used as recommended to biotinylate and isolate membrane-associated proteins. Briefly, cells were rinsed with PBS and exposed to EZ-Link Sulfo-NHS-SS-Biotin for 30 minutes at 4°C. This biotinylation reagent labels primary amines in extracellular regions of membrane-bound proteins. A quenching solution was added to prevent further biotinylation and the cells from each set of four flasks were scraped into solution and combined. Cells were rinsed with Tris-buffered saline (TBS) and lysed in buffer containing protease inhibitor cocktail (Sigma). Cells were disrupted by intermittent sonication and vortexing during a 30 minute incubation on ice. The lysate was centrifuged and 100 μl of the supernatant was retained as whole cell lysate.

Immobilised Neutravidin gel was applied to a column and washed with wash buffer. The remaining cell lysate was transferred to the column and incubated with end-over-end mixing using a rotator for 1 hour at room temperature to allow the biotinylated proteins within the lysate to bind the avidin-coated beads. Any unbound proteins were removed from the column by centrifugation, and the beads were rinsed thoroughly with wash buffer containing protease inhibitors. SDS-PAGE sample buffer (62.5 mM Tris-HCl, pH 6.8, 1% SDS, 10% glycerol) containing 50 mM DTT was added to the column and incubated for 1 hour at room temperature with end-over-end mixing to release protein bound to the avidin beads. The isolated membrane proteins were then eluted from the column by centrifugation.

The membrane protein fractions were analysed by immunoblotting. Trace amounts of bromophenol blue were added to 40 μl of each fraction which were denatured through incubation at 37°C for 30 minutes. Proteins were separated by SDS-PAGE using a 12% acrylamide gel and NIS protein was probed with mouse monoclonal anti-HA.11 antibody at a concentration of 1:1000, followed by secondary antibody, 650 ng/ml HRP-conjugated polyclonal rabbit anti-mouse immunoglobulins (Dako). Membranes were subsequently re-probed with mouse monoclonal anti-flotillin-1 antibody (BD Biosciences, Franklin Lakes, NJ) at 1:1000 to determine equal protein loading. Experiments were carried out on three separate occasions, and scanning densitometry used to quantify mean changes in expression versus flotillin controls.

Iodide-uptake assays

Iodide-uptake assays were undertaken to assess endogenous NIS function. 24 hours after transfection with either VO, PBF, M1, M2 or M3 plasmids, NaI with a final concentration of 10^{-6} moles/l and 0.05 μCi ^{125}I was added directly to FRTL-5 cell medium in each well. After 1 hour of incubation at 37°C to allow uptake of ^{125}I into the cells, medium was removed and cells were washed rapidly with Hank's balanced salt solution (HBSS) to remove unincorporated iodide. Cells were lysed in 200 μl of 2% SDS and the radioactivity of the lysate was counted for 1 minute in a gamma counter.

Exogenous NIS function in COS-7 cells was also assessed following the transient transfection of NIS-HA cDNA. 48 hours after transfection, cells were incubated with NaI with a final concentration of 10^{-5} moles/l and 0.15 μCi ^{125}I and iodide uptake determined in a similar manner to the FRTL-5 cells.

This work was supported by the Medical Research Council, UHB Charities and the Get-A-Head Charity. We thank John Morris (Mayo Graduate School of Medicine, Rochester, MN), Fedor Berditchevski

(School of Cancer Sciences, University of Birmingham, Birmingham, UK), Melissa Westwood (University of Manchester, UK) and Barbara Reaves (Department of Biology and Biochemistry, University of Bath, UK) for the kind provision of cDNAs, antibodies and expertise. Deposited in PMC for release after 6 months.

References

Ambesi-Impiombato, F. S., Parks, L. A. and Coon, H. G. (1980). Culture of hormone-dependent functional epithelial cells from rat thyroids. *Proc. Natl. Acad. Sci. USA* **77**, 3455-3459.

Arturi, F., Russo, D., Schlumberger, M., du Villard, J. A., Caillou, B., Vigneri, P., Wicker, R., Chiefari, E., Suarez, H. G. and Filetti, S. (1998). Iodide symporter gene expression in human thyroid tumors. *J. Clin. Endocrinol. Metab.* **83**, 2493-2496.

Berditchevski, F. and Odintsova, E. (2007). Tetraspanins as regulators of protein trafficking. *Traffic* **8**, 89-96.

Boelaert, K. and Franklyn, J. A. (2003). Sodium iodide symporter: a novel strategy to target breast, prostate, and other cancers? *Lancet* **361**, 796-797.

Boelaert, K., McCabe, C. J., Tannahill, L. A., Gittoes, N. J., Holder, R. L., Watkinson, J. C., Bradwell, A. R., Sheppard, M. C. and Franklyn, J. A. (2003). Pituitary tumor transforming gene and fibroblast growth factor-2 expression: potential prognostic indicators in differentiated thyroid cancer. *J. Clin. Endocrinol. Metab.* **88**, 2341-2347.

Boelaert, K., Smith, V. E., Stratford, A. L., Kogai, T., Tannahill, L. A., Watkinson, J. C., Eggo, M. C., Franklyn, J. A. and McCabe, C. J. (2007). PTTG and PBF repress the human sodium iodide symporter. *Oncogene* **26**, 4344-4356.

Caillou, B., Troalen, F., Baudin, E., Talbot, M., Filetti, S., Schlumberger, M. and Bidart, J. M. (1998). Na^+/I^- symporter distribution in human thyroid tissues: an immunohistochemical study. *J. Clin. Endocrinol. Metab.* **83**, 4102-4106.

Castro, M. R., Bergert, E. R., Beito, T. G., McIver, B., Goellner, J. R. and Morris, J. C. (1999a). Development of monoclonal antibodies against the human sodium iodide symporter: immunohistochemical characterization of this protein in thyroid cells. *J. Clin. Endocrinol. Metab.* **84**, 2957-2962.

Castro, M. R., Bergert, E. R., Beito, T. G., Roche, P. C., Ziesmer, S. C., Jhiang, S. M., Goellner, J. R. and Morris, J. C. (1999b). Monoclonal antibodies against the human sodium iodide symporter: utility for immunocytochemistry of thyroid cancer. *J. Endocrinol.* **163**, 495-504.

Chien, W. and Pei, L. (2000). A novel binding factor facilitates nuclear translocation and transcriptional activation function of the pituitary tumor-transforming gene product. *J. Biol. Chem.* **275**, 19422-19427.

De la Vieja, A., Ginter, C. S. and Carrasco, N. (2004). The Q267E mutation in the sodium/iodide symporter (NIS) causes congenital iodide transport defect (ITD) by decreasing the NIS turnover number. *J. Cell Sci.* **117**, 677-687.

De la Vieja, A., Ginter, C. S. and Carrasco, N. (2005). Molecular analysis of a congenital iodide transport defect: G543E impairs maturation and trafficking of the Na+/I-symporter. *Mol. Endocrinol.* **19**, 2847-2858.

Dohan, O., Baloch, Z., Banrevi, Z., Livolsi, V. and Carrasco, N. (2001). Rapid communication: predominant intracellular overexpression of the Na(+)/I(-) symporter (NIS) in a large sampling of thyroid cancer cases. *J. Clin. Endocrinol. Metab.* **86**, 2697-2700.

Dohan, O., De la Vieja, A., Paroder, V., Riedel, C., Artani, M., Reed, M., Ginter, C. S. and Carrasco, N. (2003). The sodium/iodide Symporter (NIS): characterization, regulation, and medical significance. *Endocr. Rev.* **24**, 48-77.

Dohan, O., Ginter, C. S. and Carrasco, N. (2005). Role of the NIS (Na+/I- symporter) carboxy terminus in iodide transport. *Thyroid* **15**, S48.

Faggiano, A., Caillou, B., Lacroix, L., Talbot, M., Filetti, S., Bidart, J. M. and Schlumberger, M. (2007). Functional characterization of human thyroid tissue with immunohistochemistry. *Thyroid* **17**, 203-211.

Gerard, A. C., Daumerie, C., Mestdagh, C., Gohy, S., De Burbure, C., Costagliola, S., Miot, F., Nollevaux, M. C., Denef, J. F., Rahier, J. et al. (2003). Correlation between the loss of thyroglobulin iodination and the expression of thyroid-specific proteins involved in iodine metabolism in thyroid carcinomas. *J. Clin. Endocrinol. Metab.* **88**, 4977-4983.

Heaney, A. P., Nelson, V., Fernando, M. and Horwitz, G. (2001). Transforming events in thyroid tumorigenesis and their association with follicular lesions. *J. Clin. Endocrinol. Metab.* **86**, 5025-5032.

James, S. R., Franklyn, J. A., Reaves, B. J., Smith, V. E., Chan, S. Y., Barrett, T. G., Kilby, M. D. and McCabe, C. J. (2008). Monocarboxylate transporter 8 (MCT8) in neuronal cell growth. *Endocrinology* **150**, 1961-1969.

Jhiang, S. M., Cho, J. Y., Ryu, K. Y., DeYoung, B. R., Smanik, P. A., McGaughy, V. R., Fischer, A. H. and Mazzaferri, E. L. (1998). An immunohistochemical study of Na^+/I^- symporter in human thyroid tissues and salivary gland tissues. *Endocrinology* **139**, 4416-4419.

Kaminsky, S. M., Levy, O., Salvador, C., Dai, G. and Carrasco, N. (1994). Na(+)-I-symport activity is present in membrane vesicles from thyrotropin-deprived non-I(-)-transporting cultured thyroid cells. *Proc. Natl. Acad. Sci. USA* **91**, 3789-3793.

Knostman, K. A., McCubrey, J. A., Morrison, C. D., Zhang, Z., Capen, C. C. and Jhiang, S. M. (2007). PI3K activation is associated with intracellular sodium/iodide symporter protein expression in breast cancer. *BMC Cancer* **7**, 137.

Kogai, T., Endo, T., Saito, T., Miyazaki, A., Kawaguchi, A. and Onaya, T. (1997). Regulation by thyroid-stimulating hormone of sodium/iodide symporter gene expression and protein levels in FRTL-5 cells. *Endocrinology* **138**, 2227-2232.

Kogai, T., Taki, K. and Brent, G. A. (2006). Enhancement of sodium/iodide symporter expression in thyroid and breast cancer. *Endocr. Relat. Cancer* **13**, 797-826.

Lazar, V., Bidart, J. M., Caillou, B., Mahe, C., Lacroix, L., Filetti, S. and Schlumberger, M. (1999). Expression of the Na^+/I^- symporter gene in human thyroid tumors: a comparison study with other thyroid-specific genes. *J. Clin. Endocrinol. Metab.* **84**, 3228-3234.

Luciani, P., Buci, L., Conforti, B., Tonacchera, M., Agretti, P., Elisei, R., Vivaldi, A., Cioppi, F., Biliotti, G., Manca, G. et al. (2003). Expression of cAMP response element-binding protein and sodium iodide symporter in benign non-functioning and malignant thyroid tumours. *Eur. J. Endocrinol.* **148**, 579-586.

Mazzaferri, E. L. and Kloos, R. T. (2001). Clinical review 128: Current approaches to primary therapy for papillary and follicular thyroid cancer. *J. Clin. Endocrinol. Metab.* **86**, 1447-1463.

Park, H. J., Kim, J. Y., Park, K. Y., Gong, G., Hong, S. J. and Ahn, I. M. (2000). Expressions of human sodium iodide symporter mRNA in primary and metastatic papillary thyroid carcinomas. *Thyroid* **10**, 211-217.

Riedel, C., Levy, O. and Carrasco, N. (2001). Post-transcriptional regulation of the sodium/iodide symporter by thyrotropin. *J. Biol. Chem.* **276**, 21458-21463.

Ries, L. A. G., Melbert, D., Krapcho, M., Stinchcomb, D. G., Howlander, N., Horner, M. J., Mariotto, A., Miller, B. A., Feuer, E. J., Altekruse, S. F. et al. (2008). *SEER Cancer Stat. Rev. 1975-2005*.

Ringel, M. D., Anderson, J., Souza, S. L., Burch, H. B., Tambascia, M., Shriver, C. D. and Tuttle, R. M. (2001). Expression of the sodium iodide symporter and thyroglobulin genes are reduced in papillary thyroid cancer. *Mod. Pathol.* **14**, 289-296.

Ryu, K. Y., Senokozlieff, M. E., Smanik, P. A., Wong, M. G., Siperstein, A. E., Duh, Q. Y., Clark, O. H., Mazzaferri, E. L. and Jhiang, S. M. (1999). Development of reverse transcription-competitive polymerase chain reaction method to quantitate the expression levels of human sodium iodide symporter. *Thyroid* **9**, 405-409.

Saez, C., Martinez-Brocca, M. A., Castilla, C., Soto, A., Navarro, E., Tortolero, M., Pintor-Toro, J. A. and Japon, M. A. (2006). Prognostic significance of human pituitary tumor-transforming gene immunohistochemical expression in differentiated thyroid cancer. *J. Clin. Endocrinol. Metab.* **91**, 1404-1409.

Saito, T., Endo, T., Kawaguchi, A., Ikeda, M., Katoh, R., Kawaoi, A., Muramatsu, A. and Onaya, T. (1998). Increased expression of the sodium/iodide symporter in papillary thyroid carcinomas. *J. Clin. Invest.* **101**, 1296-1300.

Schmutzler, C., Winzer, R., Meissner-Weigl, J. and Kohrle, J. (1997). Retinoic acid increases sodium/iodide symporter mRNA levels in human thyroid cancer cell lines and suppresses expression of functional symporter in nontransformed FRTL-5 rat thyroid cells. *Biochem. Biophys. Res. Commun.* **240**, 832-838.

Smanik, P. A., Liu, Q., Furminger, T. L., Ryu, K., Xing, S., Mazzaferri, E. L. and Jhiang, S. M. (1996). Cloning of the human sodium lodide symporter. *Biochem. Biophys. Res. Commun.* **226**, 339-345.

Smanik, P. A., Ryu, K. Y., Theil, K. S., Mazzaferri, E. L. and Jhiang, S. M. (1997). Expression, exon-intron organization, and chromosome mapping of the human sodium iodide symporter. *Endocrinology* **138**, 3555-3558.

Spitzweg, C., Joba, W., Morris, J. C. and Heufelder, A. E. (1999). Regulation of sodium iodide symporter gene expression in FRTL-5 rat thyroid cells. *Thyroid* **9**, 821-830.

Stratford, A. L., Boelaert, K., Tannahill, L. A., Kim, D. S., Warfield, A., Eggo, M. C., Gittoes, N. J., Young, L. S., Franklyn, J. A. and McCabe, C. J. (2005). Pituitary tumor transforming gene binding factor: a novel transforming gene in thyroid tumorigenesis. *J. Clin. Endocrinol. Metab.* **90**, 4341-4349.

Tanaka, K., Otsuki, T., Sonoo, H., Yamamoto, Y., Udagawa, K., Kunisue, H., Arime, I., Yamamoto, S., Kurebayashi, J. and Shimozuma, K. (2000). Semi-quantitative comparison of the differentiation markers and sodium iodide symporter messenger ribonucleic acids in papillary thyroid carcinomas using RT-PCR. *Eur. J. Endocrinol.* **142**, 340-346.

Trouttet-Masson, S., Selmi-Ruby, S., Bernier-Valentin, F., Porra, V., Berger-Dutrieux, N., Decaussin, M., Peix, J. L., Perrin, A., Bournaud, C., Orgiazzi, J. et al. (2004). Evidence for transcriptional and posttranscriptional alterations of the sodium/iodide symporter expression in hypofunctioning benign and malignant thyroid tumors. *Am. J. Pathol.* **165**, 25-34.

Turnell, A. S., Grand, R. J., Gorbea, C., Zhang, X., Wang, W., Mymryk, J. S. and Gallimore, P. H. (2000). Regulation of the 26S proteasome by adenovirus E1A. *EMBO J.* **19**, 4759-4773.

Vadysirisack, D. D., Chen, E. S., Zhang, Z., Tsai, M. D., Chang, G. D. and Jhiang, S. M. (2007). Identification of in vivo phosphorylation sites and their functional significance in the sodium iodide symporter. *J. Biol. Chem.* **282**, 36820-36828.

Van Sande, J., Massart, C., Beauwens, R., Schoutens, A., Costagliola, S., Dumont, J. E. and Wolff, J. (2003). Anion selectivity by the sodium iodide symporter. *Endocrinology* **144**, 247-252.

Wapnir, I. L., van de Rijn, M., Nowels, K., Amenta, P. S., Walton, K., Montgomery, K., Greco, R. S., Dohan, O. and Carrasco, N. (2003). Immunohistochemical profile of the sodium/iodide symporter in thyroid, breast, and other carcinomas using high density tissue microarrays and conventional sections. *J. Clin. Endocrinol. Metab.* **88**, 1880-1888.

Ward, L. S., Santarosa, P. L., Granja, F., da Assumpcao, L. V., Savoldi, M. and Goldman, G. H. (2003). Low expression of sodium iodide symporter identifies aggressive thyroid tumors. *Cancer Lett.* **200**, 85-91.

Yaspo, M. L., Aaltonen, J., Horelli-Kuitunen, N., Peltonen, L. and Lehrach, H. (1998). Cloning of a novel human putative type Ia integral membrane protein mapping to 21q22.3. *Genomics* **49**, 133-136.

Zhang, Z., Liu, Y. Y. and Jhiang, S. M. (2005). Cell surface targeting accounts for the difference in iodide uptake activity between human Na^+/I^- symporter and rat Na+/I-symporter. *J. Clin. Endocrinol. Metab.* **90**, 6131-6140.